AUCTORES
Globalize your Research

International Journal of Clinical Case Reports and Reviews
Ferydoon Khamooshi *

Open Access

Research Article

As a new Biomedical drug for the future: A Template-free Synthesis of a new poly (aniline-co-m- amino Benzenesulfonic acid) Nanobelts along with Estimation of the Exact amount of the Sulfonated Monomer Inserted in the main Copolymer Chain

Ferydoon Khamooshi [1]*, Amirreza Kheirkhah [2], Samaneh Doraji-Bonjar [3], Sahar Shabzendedar [2], Ali Reza Modarresi-Alam [2] and Habib Ghaznavi [4]

[1]Department of Chemistry, Faculty of Science, University of Zabol, Zabol, Iran.

[2]Organic and Polymer Research Laboratory, Department of Chemistry, Faculty of Science, University of Sistan and Baluchestan, Zahedan, Iran.

[3]Department of Laboratory Medical Sciences, School of Allied Medical Sciences, Zahedan University of Medical Sciences, Zahedan, Iran.

[4]Department of Pharmacology, Zahedan University of Medical Sciences, Zahedan, Iran.

***Corresponding Author:** Ferydoon Khamooshi, Department of Chemistry, Faculty of Science, University of Zabol, Zabol, Iran.

Received Date: November 22, 2024 | **Accepted Date:** December 06, 2024 | **Published Date:** January 14, 2025

Citation: Ferydoon Khamooshi, Amirreza Kheirkhah, Samaneh Doraji-Bonjar, Sahar Shabzendedar, Ali Reza Modarresi-Alam, et al, (2025), As a new Biomedical drug for the future: A Template-free Synthesis of a new poly (aniline-co-m- amino Benzenesulfonic acid) Nanobelts along with Estimation of the Exact amount of the Sulfonated Monomer Inserted in the main Copolymer Chain, *International Journal of Clinical Case Reports and Reviews*, 22(3); **DOI:10.31579/2690-4861/636**

Abstract:

In this study, a novel antibacterial nanocomposite of poly (aniline-co-m-amino benzenesulfonic acid) (NPAABS), was synthesized using a simple, green, and template-free method. The synthesis produced both salt and base forms of the nanocomposite, which were characterized using various techniques, including FT-IR, UV-Vis's spectroscopy, elemental analysis, TGA, DSC, XRD, and SEM/TEM microscopy. The results indicated that some m-amino benzenesulfonic acid acted as dopant anions, while others were incorporated into the polymer chains as monomers, confirming the successful synthesis of the copolymer. The nanocomposites exhibited nanobelt morphology, with average diameters of 38 nm for the salt form and 26 nm for the base form. Additionally, the study provided insights into the conductivity and thermal stability of the synthesized materials, revealing that the NPAABS-salt demonstrated higher conductivity compared to the NPAABS-base. Based on the results of this research, it is possible to develop new materials with improved properties and diverse applications in various fields such as sensors, supercapacitors, and biomedical materials.

Key words: nanobelt pani copolymer; template-free synthesis; new biomedical compound; polymerization mechanism; anti-bacterial properties

Highlight:

This research focuses on the synthesis of new nano-capsules of polyaniline and m- amino benzenesulfonic acid with antibacterial and medicinal properties. The nano-capsules were prepared in both salt and base forms, and their properties were analyzed using FT-IR and elemental analysis. The results show that these nano-capsules could be used in the development of biomedical drugs and antimicrobial materials.

Introduction

Recent years has witnessed a growing interest in synthesis of unidimensional nanostructures of conjugated polymers [1-3] as they are characterized with both organic conductors and low dimensional systems, with possible applications in molecular wires through polymeric conduction [4], chemical sensors [5-8], membranes of gas separation [9], supercapacitors [10, 11], and electronic and light-emitting devices [12, 13]. One of the conducting polymers that has been the subject of growing studies is PANI, mainly because of its inexpensiveness, ease of synthesis, excellent environmental stability, electrical conductivity and redox

reversibility [14-20]. PANI has also been widely employed in biosensor development, especially for biosensing glucose, peroxide, nucleic acid, cholesterol, immune cytokines, and phenols. In addition, PANI is utilized in tissue engineering applications related to cardiac, nerve, skeletal muscle, and bone tissue [21, 22]. Using a variety of methods including electrochemistry [23], surfactant assemblies [24], nanofiber seeding polymerization [25], and green synthesis [26], researchers have reported different PANI nanostructures, such as nanofibers, nanotubes, nanorods, nanoplates, and nanoparticles. Also, many copolymers of aniline and its derivatives have been synthesized with diverse morphology and their properties have been investigated [27-29]. For example, Ding et al. reported the synthesis of poly (aniline-co-m-nitroaniline) nanofibers by chemical and electrochemical polymerization [30]. The breaking stone-like structure of poly (aniline-co-ethyl-4-aminobenzoate) was synthesized using the electrochemical method by Sasikumar and Manisankar [31]. The sharp-edged rhombohedral blocks have been reported in copolymers of aniline and amino benzene sulfonic acid synthesized by the solution method with ammonium persulfate acting as the oxidant [32]. Acids and solid acids play an important role in synthetic reactions [33, 34]. In the chemical reactions of amines, both in the synthesis of amines and in the processability of amines, the presence of acidic reagents in terms of nucleophilic and oxidation-reduction mechanisms is very useful as a facilitating factor for the mechanism and reaction [35-44]. There are other instances of aniline copolymer synthesis with different morphologies, but they have not been discussed here for the sake of brevity. Since this paper describes the synthesis of a copolymer of aniline and m-amino benzene sulfonic acid with nanobelt morphology, some examples of polymers with this morphology are given below. Yu et al. synthesized the polyaniline nanobelts, flower-like and rhizoid-like nanostructures using the electrospinning method in HCl/H2SO4 solution and ammonium persulfate as the oxidant at room temperature [45]. Lan et al. presented the synthesis of polyaniline nanobelts in a simple mixture of aniline and hydrochloric acid aqueous solution with ammonium peroxydisulfate and hydrochloric acid aqueous solution at room temperature in the absence of any templates [46]. The polyaniline nanobelts were synthesized with predominant electrochemical performances by Li et al., [47]. Further, a synthesis of the polyaniline nanobelts was carried out by Li et al. in a self-assembly process by utilizing the chemical oxidative polymerization of aniline in a surfactant gel [48]. The results shown in Table 1 prove that the antibacterial activities of Polyaniline copolymers are more potent than standard antibiotics [49-55]. According to Figure 1, the antimicrobial properties of the copolymer of aniline derivatives due to the interference of the polyaniline parts of the copolymer with the potential of interaction with Electrical charges disrupt the bacterial cell membrane [52].

It causes leakage of cytoplasmic contents or its complete lysis cells and thus causes the death of the bacteria [49-52, 56-58]. To the best of our knowledge, there is no report on the synthesis of aniline copolymers and their derivatives with nanobelt morphology and this paper is the first attempt to investigate such the synthesis and morphology. This nano copolymer was synthesized using the chemical method in an HCl solution, at 45 °C and in the presence of ammonium persulfate as an oxidant. Also, we used NaOH solution to the preparation of the base form of the copolymer and eliminated the monomers which were placed as dopant molecules alongside the polymer chains. The main objective of the base-copolymer synthesis is to investigate the role of m-amino benzene sulfonic acid in copolymer composition. Thus, the FT-IR spectroscopy and elemental analysis are used to study the *m*-amino benzenesulfonic acid behavior and to calculate the true content of m-amino benzene sulfonic acid monomers entering into the polymer chains and the amount of which acted as the dopant agents. So far, there is no reported papers have used base copolymers to determine the exact and true amount of the sulfonated monomer entered into the main copolymer chains.

Antibacterial activity of PANI Copolymer film using Kirby-Bauer technique (Zone of growth inhibitation, mm)

	Zone of growth inhibitation[a] (mm)			
Test strain	PANI-b-PAA (film[b])	Gentamicin (10µg per disk)		Chloramphenicol (30µg per disk)
E. Coli	28.0 ± 1.4	19.6 ± 1.1		20.7 ± 1.5
P. aeruginosa	28.5 ± 0.7	15.6 ± 0.5		NE[c]
S. aureus	31.5 ± 0.7	20.3 ± 1.5		21.7 ± 0.6
B. Subtilis	27.5 ± 0.7	26.0 ± 1.7		22.3 ± 1.2

[a]Strong activity>16mm, moderate activity 10-16 mm, weak activity <10mm. [b]Diameter of film: 10mm, Mueller-Hinton agar plat [c]No effect

Comparison of inhibitation zone values of PANI and PANI Copolymers

	Zone of growth inhibitation (mm)	
Test strain	*E. Coli (negative type)*	*S. aureus (positive type)*
Pure PANI	10.0 ± 0.4	11.0 ± 0.5
PANI-Cellulose Copolymer	13.0 ± 0.4	16.0 ± 0.4
PANI-$Cu_{0.05}Zn_{0.95}O$ Copolymer	33.3 ± 0.0	35.9 ± 0.0
PANI-PVA-Blend Copolymer	00.0 ± 0.0	00.0 ± 0.0
PANI-PVA-Ag (15%) Copolymer	12.0 ± 0.0	15.0 ± 0.0
Present Work Copolymer	28.0 ± 1.4	31.5 ± 0.7

Table 1: Investigation and comparison of antibacterial properties of polymer and copolymers of PANI (Polyaniline)

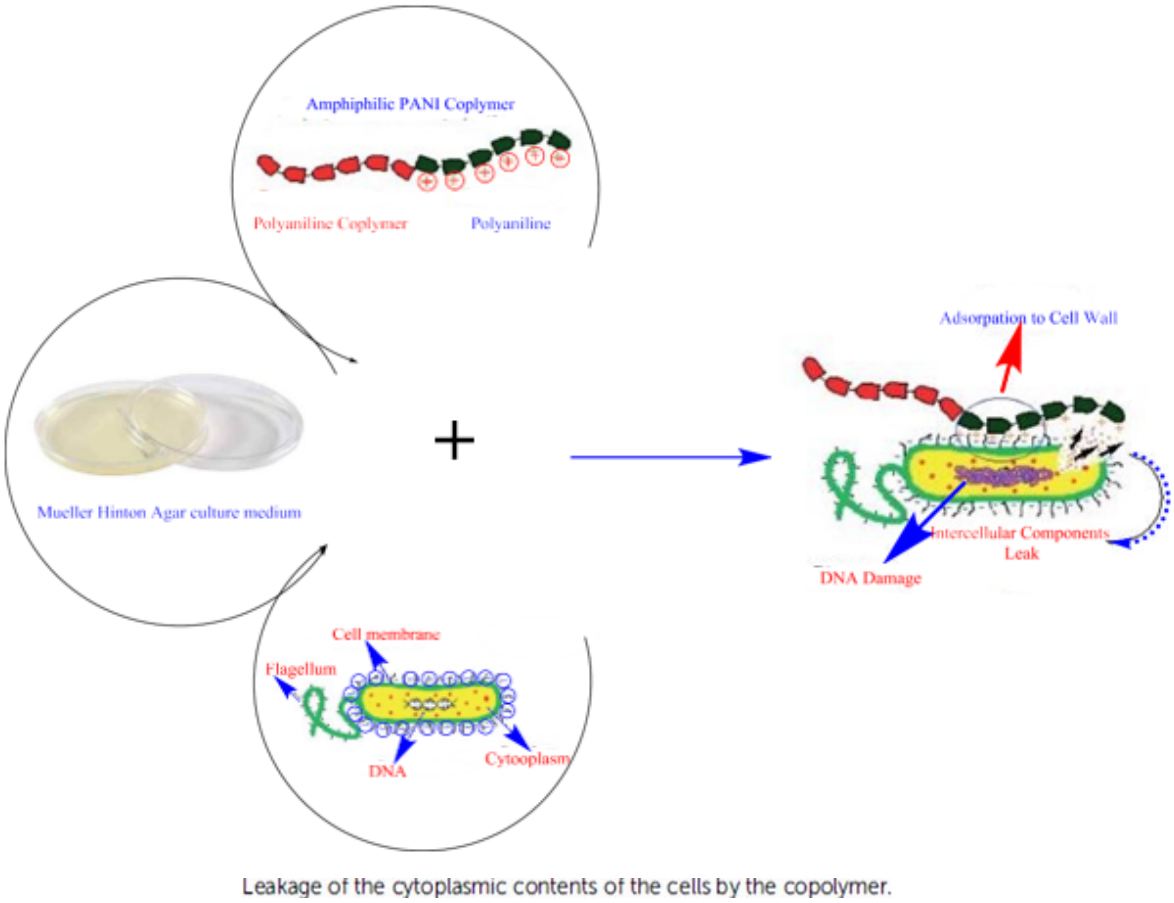

Figure 1: Anti-bio diagram of PANI-Co-Polymer antibacterial properties

Materials and Methods

Materials

All chemicals were purchased from Fluka and Merck Chemical Co. (Germany). m-Amino benzenesulfonic acid (m-ABS), ammonium persulfate (APS), HCl, methanol, sodium hydroxide, were used as received except for aniline and NMP, which was distilled to purify.

Measurements

FT-IR spectra were recorded by an FTIR-JASCO 460 spectrometer on KBr pellets over the range of 400-4000 cm-1. Ultraviolet-visible spectra were recorded in an S100 ANALYT-IKJENA SPECORD spectrophotometer using a dilute nanocomposite solution (0.20 g/dL) in NMP. The elemental analysis was carried out by a CHNS-600 Leco elemental analyzer. Thermogravimetric analysis (TGA) and Differential scanning calorimeter (DSC) were performed using the DuPont Instruments (TGA50H) analyzer at 10 C/min under an O2 atmosphere in the temperature range of 0-800°C. X-ray powder diffraction (XRD) patterns were recorded by an X-ray diffractometer (GBC MMA instrument) and Be-filtered CuKα (0.15418 nm) operated at 35.4 kV and 28 mA. The 2θ scanning range was set between 5° and 90° at a scan rate of 0.05 (°/s). Scanning electron microscopy (SEM) was recorded by a Hitachi S4160 instrument. Images of the transmission electron microscopy (TEM) were recorded by a Philips CM-10 at 100 kV. The conductivity of the sample was determined using the four-probe technique tablets (bulk no film).

Synthesis of nano poly (aniline-co-m-ABS) salt (NPAABS-salt)

In a 50-ml round-bottom flask, m-amino benzene sulfonic acid (5 mmol, 0.866 g) was dissolved in 20 ml HCl (1M) at about 60°C (to dissolve the monomer) and then the ammonium persulfate (5 mmol, 1.141 g) was added. Aniline (5mmol, 0.446 g) was added drop-wise to the reaction mixture at 45°C. The reaction mixture color changed to brown due to the onset of copolymerization and oxidation of monomers. Following 1 h of heating, the mixture color grew dark green owing to the growth of copolymer chains. After that, the mixture was heated at 45°C for 6 h and then placed at room temperature for 18 h. The collection of formed precipitate was conducted by filtration and washed with distilled water to produce a dark green powder. It was then dried for 12 h in the oven at 65-70 °C and a yield of 73% was obtained. The synthetic procedure is shown in Figure 2.

Synthesis of nano poly(aniline-co-m-ABS) base (NPAABS-base)

The mixture of NPAABS-salt (1.14 mmol, 0.15 g) and 23 ml NaOH (0.1 M) was stirred at room temperature for 72 h at a constant pH = 9-10. The precipitate was collected by filtration and washed with distilled water and then dried for 12 h in the oven at 65-70 °C. The weight and the reaction yield were about 0.058 g and 38.73%, respectively. The synthetic procedure is shown in Figure 2.

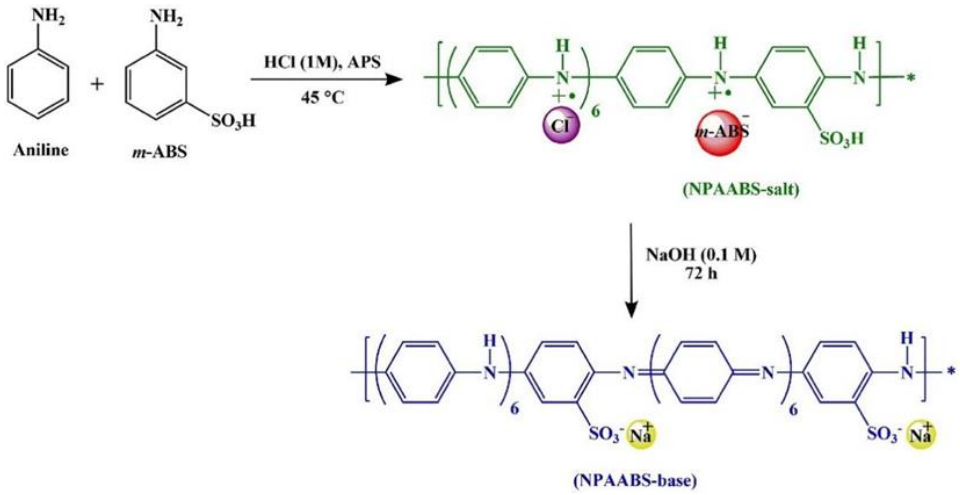

Figure 2: Synthesis of (NPAABS-salt) and (NPAABS-base)

Results and Discussion

FT-IR spectra characterization

FT-IR spectra provide useful information that confirms the formation of NPAABS-salt and NPAABS-base. Figure 3 shows the FT-IR spectra of synthesized copolymers. Absorption bands above 3200 cm^{-1} are attributed to the N–H stretching. The broad absorption bands at wavenumbers higher than 2000 cm^{-1} in the spectra of NPAABS-salt, compared to NPAABS-base, indicates that NPAABS-salt is more conductive than NPAABS-base. Hence, the conductivity of copolymers confirms the results (Section 3.4).

The spectra of NPAABS-salt and NPAABS-base exhibit main bands at 1488-1495 and 1574-1584 cm^{-1}, which correspond to C=C stretching of benzene ring and C=C and C=N stretching of quinone ring, respectively [59, 60]. The coexistence of these bands (benzenoid and quinoid) in FT-IR spectra indicates the formation of polymers.

Two other indicator bands appeared at 1171 cm^{-1} in NPAABS-salt and 1140 cm^{-1} in NPAABS-base. The former was assigned to C–H in-plane deformation of Q=NH+–B (Q and B are quinoid and benzenoid rings, respectively) or B–NH+•–B unit, which is characteristic of polaron and bipolaron states [59-61]. The latter is caused by B–NH–B and/or aromatic C–H in-plane deformation of N=Q=N. This band is characteristic of the base state. In addition, the presence of O=S=O unsymmetrical and symmetric stretching vibrations (Ar-SO_3H or –SO_3-) at 1303-1309 cm-1 and 1010-1021 cm^{-1}, respectively, and C-S unsymmetrical stretching vibration at 614 and 616 cm-1 confirms the existence of m-amino benzene sulfonic acid (m-ABS) monomer in polymer chains and the formation of copolymers in both spectra. However, the intensity of recent peaks in sulfur-bonded bonds for the base form (NPAABS-base) has declined compared to the salt form (NPAABS-salt). This indicates that some of the sulfonated monomers have been placed alongside the copolymer chains as a dopant anion to maintain electric neutrality, which was eliminated after washing with NaOH.

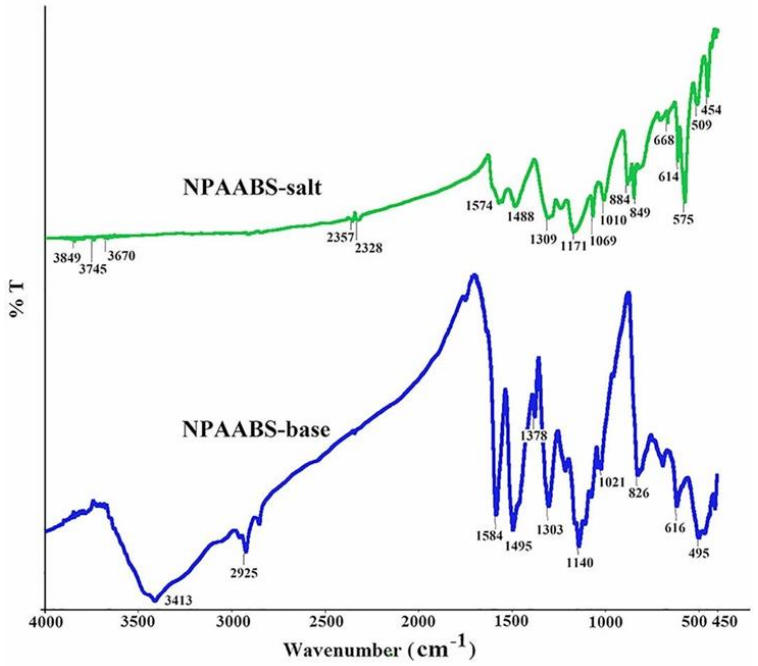

Figure 3: FT-IR spectra of NPAABS-salt and NPAABS-base

The incomplete removal of the peaks corresponding to sulfur-bonded bonds for the base form (NPAABS-base) confirms the insertion of sulfonated monomers in polymer chains and the formation of copolymers. The elemental analysis also demonstrates this decline (Section 3.3), [61-64]. The bands appearing at 849 and 826 cm^{-1} could be assigned to C–H out-of-plane bending vibration (1, 2, 4-trisubstituted ring). This suggests that copolymers have the head-to-tail coupling (para-coupling) structure of aniline units in chains [61-64].

UV-Vis spectroscopy

Figures 4a and 4b represent the UV–Vis's absorption spectra of samples in the NMP and formic acid solvents, respectively. In Figure 4a, the absorption peak at 340 nm is due to π→π* transitions of benzenoid rings, whereas the peaks at 635 and 640 nm correspond to n→π* electronic transition of the quinoid segments. These bands can be attributed to non-protonated quinoid or oxidized polyaniline base forms [65]. The NPAABS-salt in the NMP solvent (due to the presence of the basic carbonyl group in the NMP) was transformed into an NPAABS-base form and the UV-vis spectra of the NPAABS-salt and NPAABS-base were found to be identical [61-66]. The spectra of samples in the formic acid (Figure 4b) were different from their spectrum in NMP due to the nature of the solvents. The polymers were doped in the formic acid and the polaron structure was formed. Thus, p (polaron)→π* and π→p transitions appeared at 400-420 and ~800 nm, respectively.

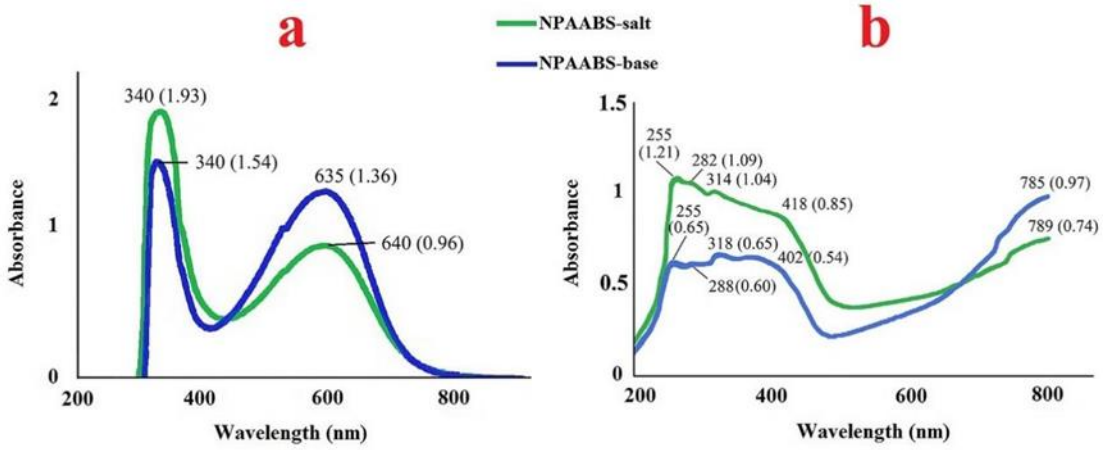

Figure 4: UV–Vis spectra of NPAABS-salt and NPAABS-base (0.02 g/L) in (a) NMP and (b) formic acid

The π→π* transition of quinoid rings was observed at 255-300 nm in both spectra. Also, the peaks at 314 and 318 nm corresponded to π →π* electronic transition of the benzenoid rings. The UV-Vis spectra of NPAABS-salt and NPAABS-base in the formic acid were identical since the NPAABS- base was doped in the formic acid and converted into the salt form [60-66].

Elemental analysis (CHN and S)

The CHNS results are consistent with the estimated and experimental data. To obtain the formula of NPAABS-salt and NPAABS-base in Table 2, we proposed a formula that was tested with computational calculations. The ratios reported in Table 2 were obtained using this formula [62]. The results of CHNS support the presence of Cl and *m*-ABS counter ions as well as the doping of NPAABS-salt chains with some *m*-ABS molecules, which were further approved by FT-IR for NPAABS-salt and NPAABS-base. As shown in Table 2, after the synthesis of NPAABS-base, the N/S ratio increased due to the elimination of *m*-ABS molecules, which acted as the dopant, and were placed alongside the polymer chains. It also indicates that not all *m*-amino benzene sulfonic acid monomers had entered into the polymer chains. The monomers which acted as dopants are then removed by adding NaOH solution. In addition, the presence of sulfur in the NPAABS base after the dedoping process confirms the formation of copolymers.

Sample	Symbol	C	H	N	S	C/N	N/S
NPAABS-Salt	Weight (%)	58.91	4.81	10.73	6.54		
	Mole	4.90	0.20	0.77	4.77	6.40	3.75
	Mole ratio	24.03	23.40	3.75	1.0		
NPAABS-Base	Weight (%)	59.86	4.74	10.16	3.72		
	Mole	4.98	4.70	0.72	0.11	6.87	6.25
	Mole ratio	42.96	40.55	6.25	1.0		

Table 2: The elementary composition of NPAABS-salt and NPAABS-base (CHN and S)

Conductivity

The conductivity of NPAABS-salt and NPAABS-base were estimated at 6.3×10^{-4} and 2.0×10^{-5} S/cm, respectively. The conductivity of samples was in the region of semi-conductive polymers, which was consistent with the doping percent. As can be seen, conductivity dropped by removing the dopant molecules in the synthesis of NPAABS-base. The conductivity of polyaniline and its derivatives soared by increasing the extent of doping [63, 66-68]. The chemical structure of the counter anion

or dopant influences the conductivity of the polyaniline [69]. Generally, the substituted polyaniline has lower conductivity compared to the original polyaniline. The existence of substituents in the polymer chains may give rise to non-planer conformations, which reduces conjugation along the backbone [60, 61, 63, 66-68]. The steric effects of the SO_3H substituent diminish the conductivity of samples in comparison with the unsubstituted polyaniline. The synthetic procedure of NPAABS-salt and NPAABS-base based on the elemental analysis is shown in Figure 2.

Thermal properties

TGA curves of synthesized nano copolymers under O_2 up to 800 °C are shown in Figure 5. The corresponding data of $T_{10\%}$, char yields (C.Y.) and

limiting oxygen indexes (LOI), computed from char yields at 800°C are depicted in Table 3. The C.Y. could be employed as a criterion for assessing the LOI of polymers based on Van Krevelen and Hoftyzer Equation1[69].

LOI = 17.5 + 0.4 C.Y.

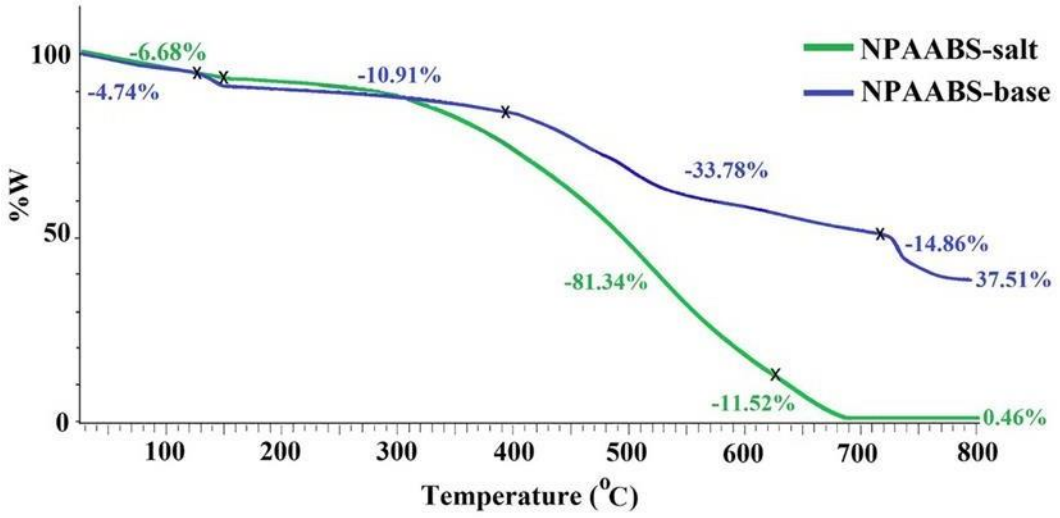

Eq. 1. Van Krevelen and Hoftyzer equation

Figure 5: TGA curves of NPAABS-salt and NPAABS-base under O_2 at a heating rate of 10 °C/min.

Sample	$T_{10\%}$ (°C)	C.Y (%)	LOI (%)
NPAABS-Salt	274	0.46	17.68
NPAABS-Base	222	37.51	32.5

Table 3: Thermal properties of NPAABS-salt and NPAABS-base

Overall, a polymer LOI of higher than 26% was seen as self-extinguishable and the calculated LOI of NPAABS-salt is 32.5%. Hence, it was assigned to this category. The $T_{10\%}$ values of NPAABS-salt and NPAABS-base were 274 °C and 222 °C, respectively. It reveals that their high thermal stability depends on the chemical structure of the repeating unit. In both curves, the first weight loss could be ascribed to water withdrawal or breaking of the intermolecular hydrogen bonds at temperatures lower than 150°C. The second step was between 150-630 °C (-81.34%) in the NPAABS-salt curve, and the second and third weight losses of about 10.91% between 160 °C and 390 °C and 33.78% between 390 °C and 720 °C in NPAABS-base curve were assigned to the loss of HCl from the complex in the polymer chain and the thermal decomposition of polymers at high temperature as well as the removal of SO_3 group from the polymer backbone and NO_2 and CO_2 groups, respectively (also decomposition of the *m*-aminobenzene sulfonic acid as dopant molecules for NPAABS-salt). The slope of NPAABS-base weight loss grew sharper over 720 °C with a loss of about 14.86%, which can be attributed to the binary eutectic point of a mixture of NaCl-Na_2SO_{4d}.

This is a phase transition (melting point) of the NaCl-Na_2SO_4 binary system, as shown by the DSC curve in Figure 6. Indeed, the C.Y of about 38% in the NPAABS-base is related to NaCl and Na_2SO_4. The crystalline structure of NPAABS-base is caused by the presence of these salts (see Section 3.6).

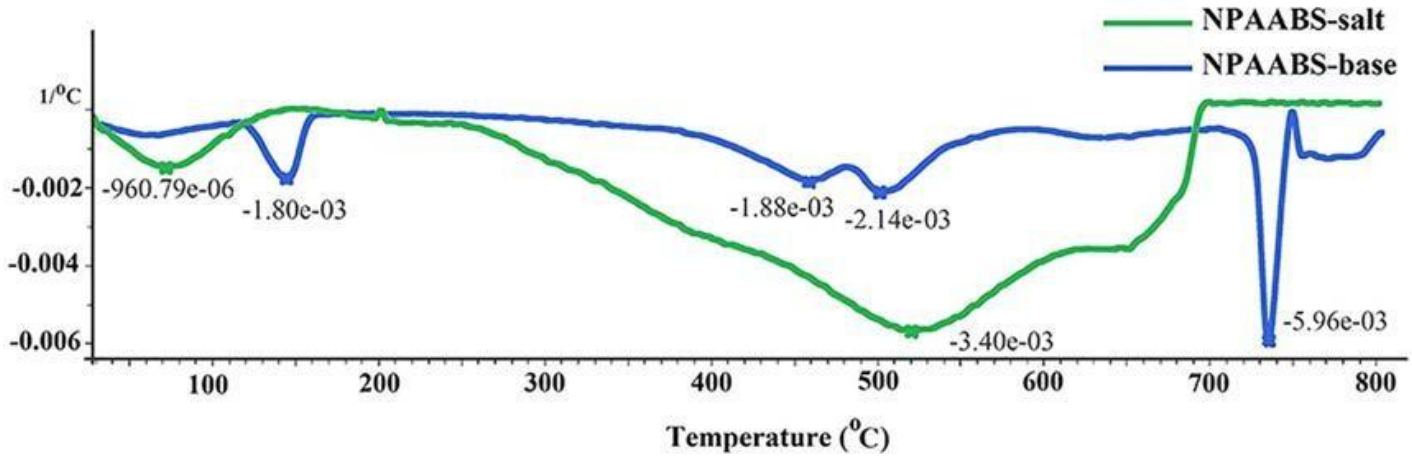

Figure 6: DSC curves of NPAABS-salt and NPAABS-base

X-ray diffraction (XRD) analysis

In this study, the X-ray diffraction (XRD) technique was utilized to

investigate the crystalline nature of NPAABS-salt and NPAABS-base. The XRD patterns of synthesized samples are shown in Figure 7. According to XRD patterns, NPAABS-salt has an amorphous structure while NPAABS-base has a crystal structure induced by sharp peaks (at 2θ = 23.5°, 26.5°, 29.5°, 31.5°, 33°, 34.5°, 39.5°, 45.5° and 48°), which are produced by the presence of NaCl and Na_2SO_4 [70-73]. The latter was confirmed by TGA and DSC in the last Section.

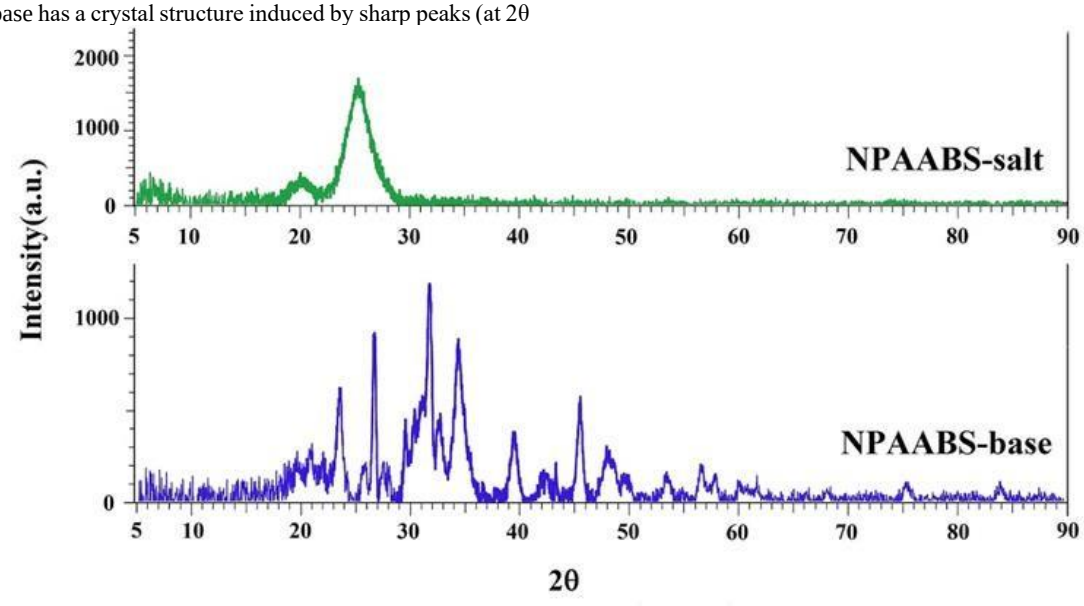

Figure 7: X-ray diffraction patterns of NPAABS-salt and NPAABS-base

SEM and TEM analysis

The size and morphology of the samples were characterized by SEM and TEM microscopies. As shown in Figure 8, both copolymers had nanobelt morphology of approximately the same size, as confirmed by the TEM images. In the SEM images, the average diameter size was about 80 nm and 87 nm for NPAABS-salt and NPAABS-base, respectively. As can be observed, the average diameter of NPAABS-salt in TEM images was ~ 38 nm, and the average length of nanobelts was ~ 101 nm. These values were ~ 26 and 216 nm for NPAABS-base nanobelts, respectively. It can be concluded
that the extended length of NPAABS-base nanobelts is due to the expansion of polymer chains (expanded-coil) [41] caused by the removal of sulfonated monomers, which were placed as dopant alongside the polymer chains as shown in Figure 10. It reveals how the addition of NaOH can change morphology.

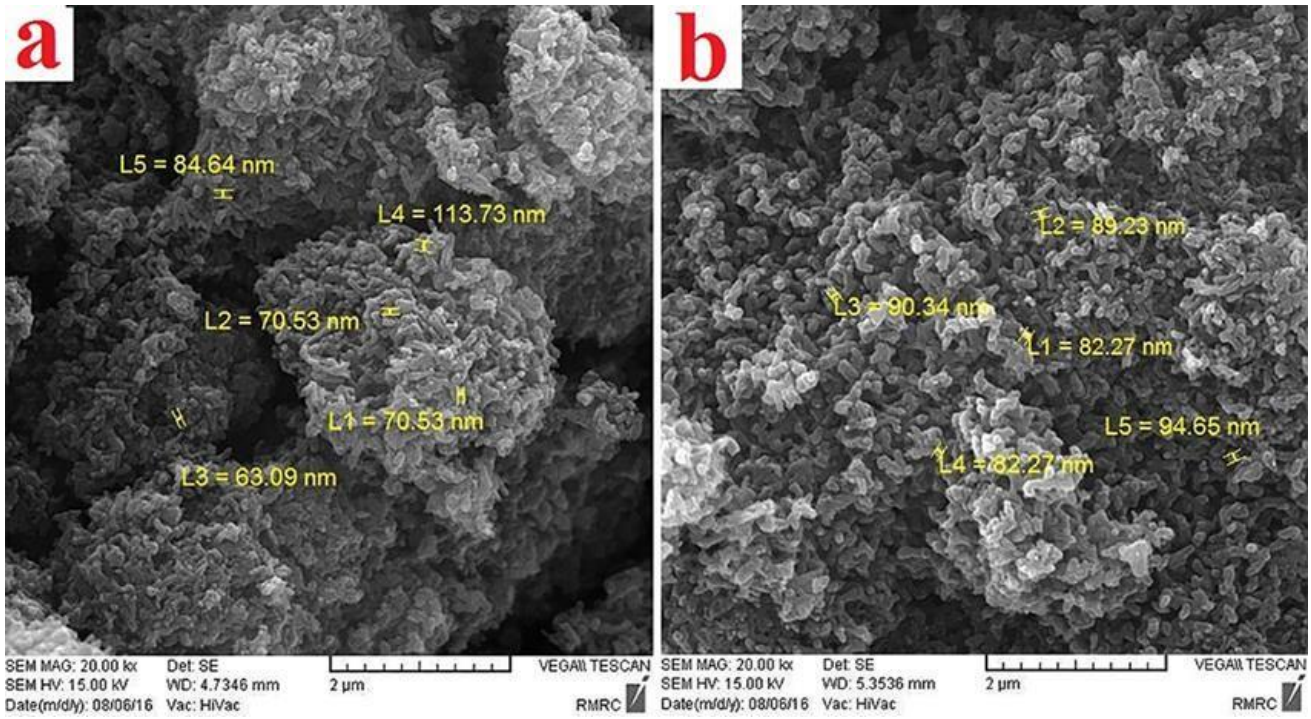

Figure 8: SEM images of (a) NPAABS-salt and (b) NPAABS-base.

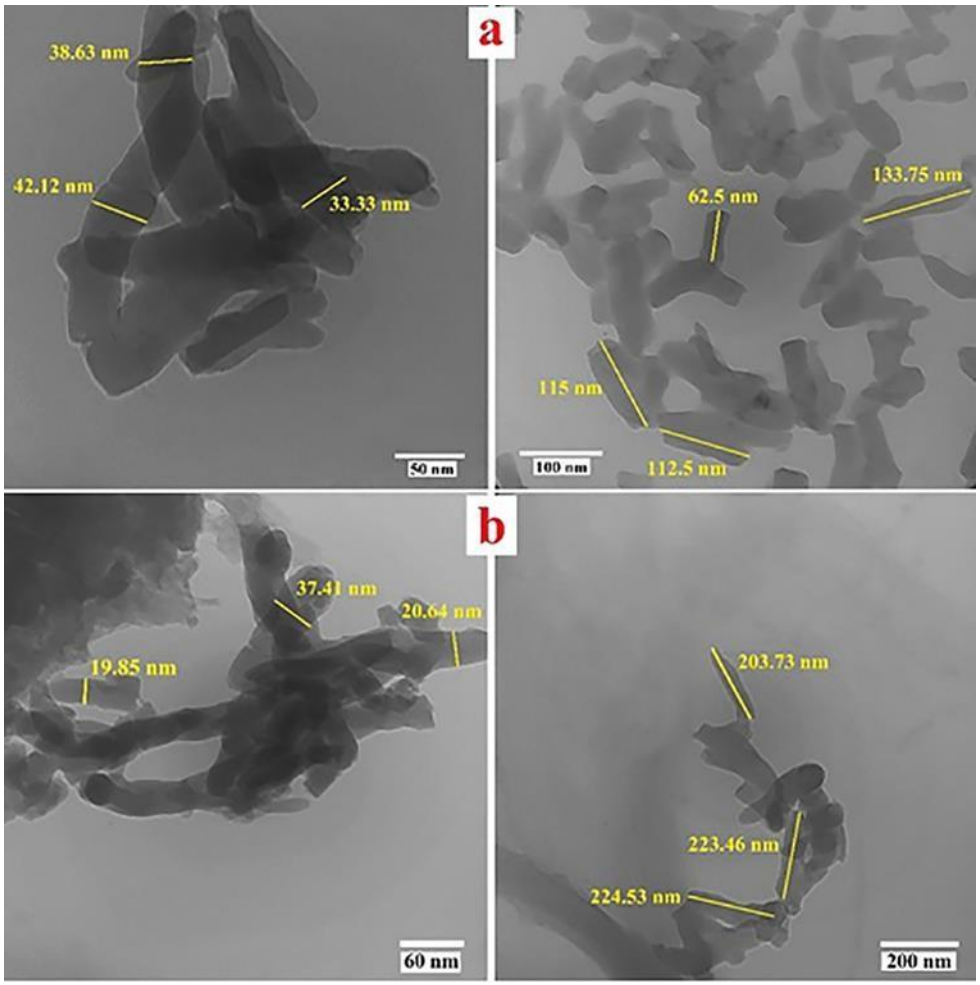

Figure 9: TEM images of (a) NPAABS-salt and (b) NPAABS base

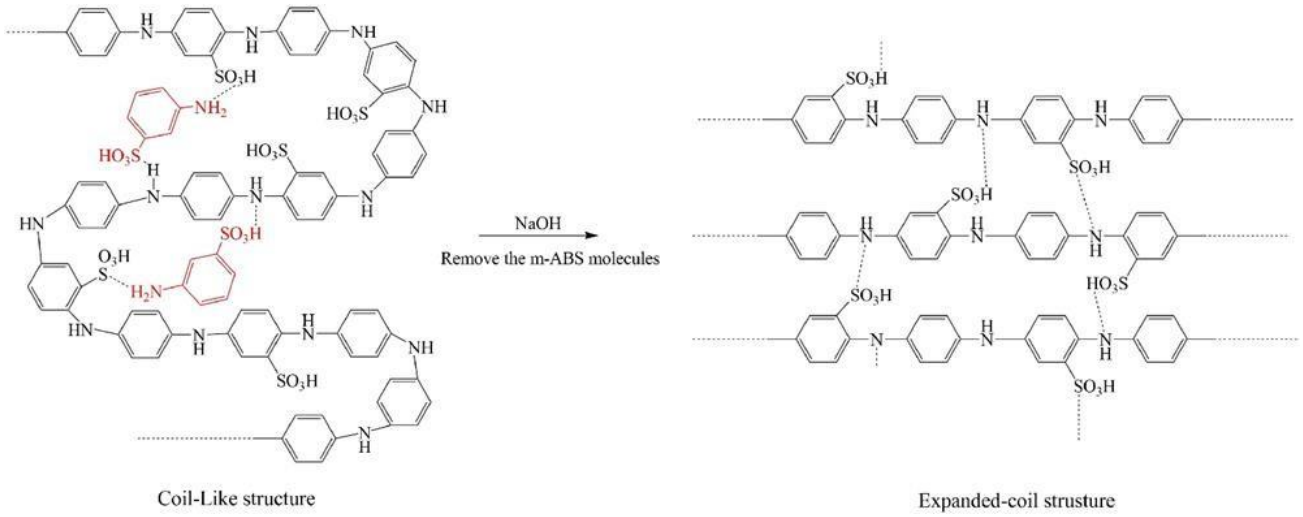

Figure 10: Schematic structure of the coil-like polymer chains and the formation of the expanded coil

Anti-Bacterial and Biomedical Properties

According the Table 1, The future of biomedicine looks very promising due to the unique properties of nanocarriers synthesized from polyaniline and m-amino benzenesulfonic acid (NPAABS). These nanocarriers, as new biomedical drugs, can be effective in treating diseases and infections, especially because of their significant antibacterial properties. Furthermore, due to their nanostructured nature, nanocarriers have the potential to be used in tissue engineering and the development of targeted drugs. These materials can be used in cardiac, neural, and muscular tissues. Additionally, the results show that these nanocarriers can also be used in chemical and electronic sensors, which contributes to the development of new technologies in the medical and pharmaceutical fields [49-52, 54, 56-58, 74]. Ultimately, this research presents a simple and effective method for synthesizing semiconductor nanocarriers with

biomedical and pharmaceutical properties, which can help in the development of new materials in the medical and pharmaceutical fields.

Conclusions

In this study, the synthesis of the new nano copolymers of aniline and *m*-amino benzenesulfonic acid was investigated under the solution condition with the nanobelt morphology using the template-free method. Another goal of this study was to prepare both salt and base forms of copolymers to determine the true and exact amounts of sulfonated monomers entering the copolymer chains. According to the N/S ratio of CHNS analysis and FT-IR spectra of copolymers, it appears that not all *m*-amino benzene sulfonic acid monomers have succeeded enter into the polymer chains. That is, some acted as a dopant and were thus removed from the polymer chains after washing with the NaOH solution. This comparison was done for the first time. In none of the reported papers base- copolymers have been used to determine the number of sulfonated monomers entered into the main copolymer chains. For the first time, we demonstrated that not all sulfonated monomers are included in the copolymer matrix, and some of them act as dopant anions and are placed alongside the polymer chains. Furthermore, how the addition of NaOH can change morphology. This research investigates the biomedical and pharmaceutical properties of a new nanocarrier made of polyaniline and *m*-amino benzenesulfonic acid (NPAABS). The synthesized nanocarriers have significant antibacterial properties that can be used in the development of biomedical drugs and antimicrobial materials. The results show that these nanocarriers can be effective as a new biomedical drug in the treatment of diseases and infections. Moreover, due to their nanostructured nature, nanocarriers can be used in tissue engineering applications, especially in cardiac, neural, and muscular tissues. Additionally, these nanocarriers have high thermal and electrical stability, making them suitable for chemical and electronic sensors.

As a result, this paper offers an exhaustive set of strategies, including the synthesis of the semi- conducting nano copolymer with nanobelt morphology, along with simple, effective, and inexpensive preparation and true and exact estimation of the amount of sulfonated monomer entering the copolymer chain; and In conclusion, this research presents a simple and effective method for synthesizing semiconductor nanocarriers with biomedical and pharmaceutical properties, which can aid in the development of new materials in the medical and pharmaceutical fields.

Acknowledgments

The Graduate Education Council of Sistan and Baluchistan University, Zabol University, and Zahedan University of Medical Science supported this research.

Conflicts of Interest

The authors declare no conflict of interest.

References

1. A. Eftekhari, (2010). Nanostructured Conductive Polymers.
2. H.D. Tran, J.M. D'Arcy, Y. Wang, P.J. Beltramo, V.A. Strong, R.B. Kaner. (2011). The oxidation of aniline to produce “polyaniline”: a process yielding many different nanoscale structures. *Journal of Materials Chemistry*;21(11):3534-3550.
3. A. Mirabedini, J. Foroughi, G.G. Wallace. (2016). Developments in conducting polymer fibres: from established spinning methods toward advanced applications. *RSC Advances*;6(50):44687-44716.
4. C.-G. Wu, T. Bein. (1994). Conducting Polyaniline Filaments in a Mesoporous Channel Host. *Science*;264(5166):1757-1759.
5. J. Huang, S. Virji, B.H. Weiller, R.B. Kaner. (2003). Polyaniline Nanofibers: Facile Synthesis and Chemical Sensors. *Journal of the American Chemical Society*;125(2):314-315.
6. J. Janata, M. Josowicz. (2003). Conducting polymers in electronic chemical sensors. *Nature Materials*;2(1):19-24.
7. S. Virji, J. Huang, R.B. Kaner, B.H. Weiller. (2004). Polyaniline Nanofiber Gas Sensors: Examination of Response Mechanisms. *Nano Letters*;4(3):491-496.
8. H. Liu, J. Kameoka, D.A. Czaplewski, H.G. Craighead. (2004). Polymeric Nanowire Chemical Sensor. *Nano Letters*;4(4):671-675.
9. J. Yang, S.M. Burkinshaw, J. Zhou, A.P. Monkman, P.J. Brown. (2003). Fabrication and Characteristics of 2-Acrylamido-2-methyl-1-propanesulfonic Acid-Doped Polyaniline Hollow Fibers. *Advanced Materials*;15(13):1081-1084.
10. H. Liu, M. Han, J. Zuo, X. Deng, W. Lu, et al., (2019). Heteroatom-doped hollow carbon spheres made from polyaniline as an electrode material for supercapacitors. *RSC Advances*;9(28):15868-15873.
11. T. Wang, H. Sun, T. Peng, B. Liu, Y. Hou, B. Lei. (2020). Preparation and characterization of polyaniline/p-phenylenediamine grafted graphene oxide composites for supercapacitors. *Journal of Molecular Structure*; 1221:128835.
12. L. Liang, J. Liu, J.C.F. Windisch, G.J. Exarhos, Y. Lin. (2002). Direct Assembly of Large Arrays of Oriented Conducting Polymer Nanowires. *Angewandte Chemie International Edition*;41(19):3665-3668.
13. K. Deb, A. Bera, B. Saha. (2016). Tuning of electrical and optical properties of polyaniline incorporated functional paper for flexible circuits through oxidative chemical polymerization. *RSC Advances*;6(97):94795-94802.
14. T. Sen, S. Mishra, N.G. Shimpi. (2016). Synthesis and sensing applications of polyaniline nanocomposites: a review. *RSC Advances*;6(48):42196-42222.
15. H. Mi, X. Zhang, X. Ye, S. Yang. (2008). Preparation and enhanced capacitance of core–shell polypyrene/polyaniline composite electrode for supercapacitors. *Journal of Power Sources*;176(1):403-409.
16. S.R. Sivakkumar, W.J. Kim, J.-A. Choi, D.R. MacFarlane, M. Forsyth, D.-W. Kim. (2007). Electrochemical performance of polyaniline nanofibres and polyaniline/multi-walled carbon nanotube composite as an electrode material for aqueous redox supercapacitors. *Journal of Power Sources*;171(2):1062-1068.
17. H. Mi, X. Zhang, S. An, X. Ye, S. Yang. (2007). Microwave-assisted synthesis and electrochemical capacitance of polyaniline/multi-wall carbon nanotubes composite. *Electrochemistry Communications*;9(12):2859- 2862.
18. K.S. Ryu, K.M. Kim, N.-G. Park, Y.J. Park, S.H. Chang. (2002). Symmetric redox supercapacitor with conducting polyaniline electrodes. *Journal of Power Sources*;103(2):305-309.
19. J.H. Park, O.O. Park. (2002). Hybrid electrochemical capacitors based on polyaniline and activated carbon electrodes. *Journal of Power Sources*;111(1):185-190.
20. L.R. de Oliveira, L. Manzato, Y.P. Mascarenhas, E.A. Sanches. (2017). The influence of heat treatment on the semi-crystalline structure of polyaniline Emeraldine-salt form. *Journal of Molecular Structure*; 1128:707-717.
21. P. Chaubisa, D. Dharmendra, Y. Vyas, P. Chundawat, N.K. Jangid, C. Ameta. (2024). Synthesis and

characterization of PANI and PANI-indole copolymer and study of their antimalarial and antituberculosis activity. *Polymer Bulletin*;81(4):3333-3353.

22. L. Karthikeyan, B. Rithisa, S. Min, H. Hong, H. Kang, R. Thangam, R. Vivek. (2024). Multimodal biomedical utility of polyaniline-based supramolecular nanomaterials. *Chemical Engineering Journal*; 493:152530.
23. J. Liu, Y. Lin, L. Liang, J.A. Voigt, D.L. Huber, Z.R. Tian, E. Coker, B. McKenzie, M.J. McDermott. (2003). Templateless Assembly of Molecularly Aligned Conductive Polymer Nanowires: A New Approach for Oriented Nanostructures. *Chemistry – A European Journal*;9(3):604-611.
24. S. Xing, Y. Chu, X. Sui, Z. Wu. (2005). Synthesis and characterization of polyaniline in CTAB/hexanol/water reversed micelle. *Journal of Materials Science*;40(1):215-218.
25. X. Zhang, S.K. Manohar. (2004). Polyaniline nanofibers: chemical synthesis using surfactants. *Chemical Communications*. (20):2360-2361.
26. S. Tanwar, J.-a.A. Ho, (2015). Green Synthesis of Novel Polyaniline Nanofibers: Application in pH Sensing, *Molecules*, pp. 18585-18596.
27. Y. Liao, V. Strong, W. Chian, X. Wang, X.-G. Li, R.B. Kaner. (2012). Sulfonated Polyaniline Nanostructures Synthesized via Rapid Initiated Copolymerization with Controllable Morphology, Size, and Electrical Properties. *Macromolecules*;45(3):1570-1579.
28. H.R. Abd El-Mageed, H.M. Abd El-Salam, M.K. Abdel-Latif, F.M. Mustafa. (2012). Preparation and spectroscopic properties, density functional theory calculations and nonlinear optical properties of poly (acrylic acid-co- acrylamide)-graft-polyaniline. *Journal of Molecular Structure*. 2018; 1173:268-279.
29. B.S. Rathore, N.P.S. Chauhan, S. Jadoun, S.C. Ameta, R. Ameta. (2021). Synthesis and characterization of chitosan-polyaniline-nickel (II) oxide nanocomposite. *Journal of Molecular Structure*; 1242:130750.
30. L. Ding, Q. Li, D. Zhou, H. Cui, R. Tang, J. Zhai. (2012). Copolymerization of aniline with m-nitroaniline and removal of m-nitroaniline from aqueous solutions using a polyaniline-modified electrode: A comparative study. *Electrochimica Acta*; 77:302-308.
31. R. Sasikumar, P. Manisankar. (2011). Electrochemically synthesized nano size copolymer, poly (aniline-co-ethyl 4-aminobenzoate) and its spectroelectrochemical studies. *Polymer* ;52(17):3710-3716.
32. B.C. Roy, M.D. Gupta, L. Bhowmik, J.K. Ray. (1999). Studies on water soluble conducting polymer: Aniline initiated polymerization of m-aminobenzene sulfonic acid. *Synthetic Metals*;100(2):233-236.
33. P. Salehi, M. Ali Zolfigol, F. Shirini, M. Baghbanzadeh. (2006). Silica Sulfuric Acid and Silica Chloride as Efficient Reagents for Organic Reactions. *Current Organic Chemistry*;10(17):2171-2189.
34. A.R. Sardarian, I. Dindarloo Inaloo, A.R. Modarresi-Alam, E. Kleinpeter, U. Schilde. (2019). Metal-Free Regioselective Monocyanation of Hydroxy-, Alkoxy-, and Benzyloxyarenes by Potassium Thiocyanate and Silica Sulfuric Acid as a Cyanating Agent. *The Journal of Organic Chemistry*;84(4):1748-1756.
35. A.R. Modarresi-Alam, F. Khamooshi. (2004). A One-Pot Synthesis of Aryl N-*(4-methylphenylsulfonyl) +-N-(triphenylphosphoranylidene) imidocarbamates from 5 Aryloxytetrazoles. Synthetic Communications ;34(1):129-135.
36. F. Khamooshi, A.R. (2010). Modarresi-Alam. Solvent-free preparation of arylaminotetrazole derivatives using aluminum (III) hydrogensulfate as an effective catalyst. *Chinese Chemical Letters*;21(8):892-896.
37. A.R. Modarresi-Alam, F. Khamooshi, M. Rostamizadeh, H. Keykha, M. Nasrollahzadeh, et al., (2007). Dynamic 1H NMR spectroscopic study of the restricted SN rotation in aryl-N-(arylsulfonyl)-N (triphenylphosphoranylidene) imidocarbamates. *Journal of Molecular Structure*.;841(1):61-66.
38. F. Khamooshi, B. Haghighi-KJ, R. Aryan, A.R. Modarresi-Alam, A.R. Rezvani, et al., (2014). Solvent-free Preparation of 5-Aryloxytetrazoles via [2+3] Cycloaddition of Cyanates and Sodium Azide Using Silica Supported Sulfuric Acid as an Effective Heterogeneous Catalyst. *Chemistry of Heterocyclic Compounds*;49(10):1464-1468.
39. F. Khamooshi, S.M. Mousavi, S. Doraji-Bonjar, M. Zolfigol. (2022). Anti-HIV Drugs Study: Study of NNRTIs Function and Overview Synthesis of Specific and Rare Aryloxy Tetrazoles Derivatives as NNRTIs and Anti-HIV Drug. *Medicon Pharmaceutical Sciences*;2(3):04-10. Epub April 2022.
40. F. Khamooshi, A.S. Akinnawo, S. Doraji-Bonjar, A.R. (2024). Modarresi-Alam. Mitragynine Chemistry: Extraction, Synthesis, and Clinical Effects. *Chemistry Africa*.
41. F. Khamooshi, S. Doraji-Bonjar, A.S. Akinnawo, H. Ghaznavi, A.R. Salimi-Khorashad, M.J. Khamooshi. (2023). Dark Classics in Chemical Neuroscience: Comprehensive Study on the Biochemical Mechanisms and Clinical Implications of Opioid Analgesics. *Chemical Methodologies*;7(12):964-993.
42. A.R. Modarresi-Alam, F. Khamooshi, M. Nasrollahzadeh, H.A. Amirazizi. (2007). Silica supported perchloric acid (HClO4–SiO2): an efficient reagent for the preparation of primary carbamates under solvent-free conditions. *Tetrahedron*;63(36):8723-8726.
43. A.R. Modarresi-Alam, M. Nasrollahzadeh, F. Khamooshi. (2007). Solvent-free preparation of primary carbamates using silica sulfuric acid as an efficient reagent. ARKIVOC;2007(16):238-245.
44. N. Zhang, D. Song, W. Chen, S. Zhang, P. Zhang, N. Zhang, S. Ma. (2021). Modification of 5- methyl philanthropism from benzothiazoles to indoles as potent FtsZ inhibitors: Broadening the antibacterial spectrum toward vancomycin-resistant enterococci. *European Journal of Medicinal Chemistry*; 224:113723.
45. Q.Z. Yu, Y. Li, M. Wang, H.Z. Chen. (2008). Polyaniline nanobelts, flower-like and rhizoid-like nanostructures by electrospinning. *Chinese Chemical Letters* ;19(2):223-226.
46. Z. Lan, J. Wu, S. Gao, J. Lin, M. Huang, X. Chen. (2014). Template-free synthesis of polyaniline nanobelts as a catalytic counter electrode in dye-sensitized solar cells. *Polymers for Advanced Technologies*;25(3):343-346.
47. G.-R. Li, Z.-P. Feng, J.-H. Zhong, Z.-L. Wang, Y.-X. Tong. (2010). Electrochemical Synthesis of Polyaniline Nanobelts with Predominant Electrochemical Performances. *Macromolecules*;43(5):2178-2183.
48. G. Li, H. Peng, Y. Wang, Y. Qin, Z. Cui, Z. Zhang. (2004). Synthesis of Polyaniline Nanobelts. *Macromolecular Rapid Communications*;25(18):1611-1614.
49. N. Bagheri, M. Mansour Lakouraj, S.R. Nabavi, H. Tashakkorian, M. Mohseni. (2020). Synthesis of bioactive polyaniline-b-polyacrylic acid copolymer nanofibrils as an

effective antibacterial and anticancer agent in cancer therapy, especially for HT29 treatment. *RSC Advances*;10(42):25290-25304.

50. M.S. Lashkenari, H. Eisazadeh. (2014). Chemical Copolymerization and Characterization of Colloidal Poly (aniline- co-3-aminobenzoic acid) as a High-Performance Antibacterial Polymer. *Advances in Polymer Technology*;33(S1).
51. C. Dhivya, S.A.A. Vandarkuzhali, N. Radha. (2019). Antimicrobial activities of nanostructured polyanilines doped with aromatic nitro compounds. *Arabian Journal of Chemistry*;12(8):3785-3798.
52. A. Shalini, R. Nishanthi, P. Palani, V. Jaisankar. (2016). One pot synthesis, characterization of polyaniline and cellulose/polyaniline nanocomposites: application towards in vitro measurements of antibacterial activity. Materials Today: Proceedings;3(6):1633-1642.
53. H. Wang, M. Niu, T. Xue, L. Ma, X. Gu, G. Wei, F. Li, C. Wang. (2022). Development of antibacterial peptides with efficient antibacterial activity, low toxicity, high membrane disruptive activity and a synergistic antibacterial effect. *Journal of Materials Chemistry* B;10(11):1858-1874.
54. *54+ N. Perin, L. Hok, A. Beč, L. Persoons, E. Vanstreels, et al., (2021). N-substituted benzimidazole acrylonitriles as in vitro tubulin polymerization inhibitors: Synthesis, biological activity and computational analysis. *European Journal of Medicinal Chemistry*; 211:113003.
55. H. Zhu, H. Sun, Y. Liu, Y. Duan, J. Liu, et al., (2020). synthesis and biological evaluation of vinyl selenone derivatives as novel microtubule polymerization inhibitors. *European Journal of Medicinal Chemistry*; 207:112716.
56. K.P. Jotiram, R.G.S.V. Prasad, V.S. Jakka, R.S.L. Aparna, A.R. Phani. (2012). Antibacterial Activity of Nanostructured Polyaniline Combined with Mupirocin. *Nano Biomedicine and Engineering*;4(3):144-149.
57. X. Liang, M. Sun, L. Li, R. Qiao, K. Chen, Q. Xiao, F. Xu. (2012). Preparation and antibacterial activities of polyaniline/Cu0.05Zn0.95O nanocomposites. *Dalton Transactions*;41(9):2804-2811.
58. M. Ghaffari-Moghaddam, H. Eslahi. (2014). Synthesis, characterization and antibacterial properties of a novel nanocomposite based on polyaniline/polyvinyl alcohol/Ag. *Arabian Journal of Chemistry*;7(5):846-855.
59. M. Trchová, J. Stejskal. (2011). Polyaniline: The infrared spectroscopy of conducting polymer nanotubes (IUPAC Technical Report);83(10):1803-1817.
60. F. Movahedifar, A.R. (2016). Modarresi-Alam. The effect of initiators and oxidants on the morphology of poly [(±)-2-(sec-butyl) aniline] a chiral bulky substituted polyaniline derivative. *Polymers for Advanced Technologies*;27(1):131-139.
61. A.R. Modarresi-Alam, H.A. Amirazizi, F. Movahedifar, A. Farrokhzadeh, G.R. Asli, H. Nahavandi. (2015). The first report of polymerization and characterization of aniline bearing chiral alkyl group on ring via covalent bond; poly[(±)-2-(sec-butyl) aniline]. *Journal of Molecular Structure*; 1083:17-26.
62. A. Farrokhzadeh, A.R. (2016). Modarresi-Alam. Complete doping in solid-state by silica-supported perchloric acid as dopant solid acid: Synthesis and characterization of the novel chiral composite of poly [(±)-2- (sec- butyl) aniline]. *Journal of Solid-State Chemistry*; 237:258-268.
63. A.R. Modarresi-Alam, S. Zafari, A.R. Miandashti. (2015). A facile preparation method for synthesis of silica sulfuric acid/poly(o-methoxyaniline) core–shell nanocomposite. *Polymers for Advanced Technologies*;26(6):645-657.
64. J.M. Guerrero, A. Carrillo, M.L. Mota, R.C. Ambrosio, F.S. Aguirre, (2019). Purification and Glutaraldehyde Activation Study on HCl-Doped PVA–PANI Copolymers with Different Aniline Concentrations, *Molecules*.
65. A.G. MacDiarmid, A.J. Epstein. (1994). The concept of secondary doping as applied to polyaniline. Synthetic Metals;65(2):103-116.
66. M.S. Freund, B.A. Deore, (2007). Self-doped conducting polymers, John Wiley & Sons.
67. S. Bhadra, D. Khastgir, N. Singha, J. Lee. (2009). Progress in preparation, processing and applications of polyaniline. *Progress in Polymer Science*; 34:783-810.
68. E.T. Kang, K.G. Neoh, K.L. Tan. (1998). Polyaniline: A polymer with many interesting intrinsic redox states. *Progress in Polymer Science*;23(2):277-324.
69. T. Fujisaki, K. Kashima, S. Serrano-Luginbühl, R. Kissner, D. Bajuk-Bogdanović, et al., (2019). Effect of template type on the preparation of the emeraldine salt form of polyaniline (PANI-ES) with horseradish peroxidase isoenzyme C (HRPC) and hydrogen peroxide. *RSC Advances*;9(57):33080-33095.
70. K. Linnow, A. Zeunert, M. Steiger. (2006). Investigation of Sodium Sulfate Phase Transitions in a Porous Material Using Humidity- and Temperature-Controlled X-ray Diffraction. *Analytical Chemistry*;78(13):4683- 4689.
71. C. Rodriguez-Navarro, L. Linares-Fernandez, E. Doehne, E. Sebastian. (2002). Effects of ferrocyanide ions on NaCl crystallization in porous stone. *Journal of Crystal Growth* ;243(3):503-516.
72. F. Nurjaman, A.S. Handoko, F. Bahfie, W. Astuti, B. Suharno. (2021). Effect of modified basicity in selective reduction process of limonitic nickel ore. *Journal of Materials Research and Technology*; 15:6476-6490.
73. J.B.F.d.O. Barauna, C.S. Pereira, I.A. Gonçalves, J.d.O. Vitoriano, C. Alves. (2017). Sodium chloride crystallization by electric discharge in brine. *Materials Research*;20(Suppl 2):215-220.
74. Y.-Y. Shao, Y. Yin, B.-P. Lian, J.-F. Leng, Y.-Z. Xia, L.-Y. Kong. (2020). Synthesis and biological evaluation of novel shikonin-benzo[b]furan derivatives as tubulin polymerization inhibitors targeting the colchicine binding site. *European Journal of Medicinal Chemistry*; 190:112105.

DOI:10.31579/2690-4861/636